Separated Oscillatory Field Measurement of Hydrogen $2S_{1/2}$-$2P_{3/2}$ Fine Structure Interval

E. W. Hagley* and F. M. Pipkin†
Lyman Laboratory of Physics, Harvard University, Cambridge, Massachusetts 02138
(Received 20 October 1993)

The $2S_{1/2}$-$2P_{3/2}$ interval in hydrogen has been measured using a fast atomic beam and a separated oscillatory field technique at a beam energy of 96.5 keV using standard X-band waveguides as interaction regions. The experimental value for the $2S_{1/2}$-$2P_{3/2}$ hydrogen fine structure interval is 9911.200(12) MHz. This implies a Lamb shift of 1057.839(12) MHz, in fair agreement with the theoretical value of 1057.866(5) MHz that was calculated using the smaller of the two discrepant values of the proton radius in the literature.

PACS numbers: 35.10.Fk, 06.20.Jr, 32.30.Bv

Using a separated oscillatory field (SOF) technique the $2S_{1/2}$-$2P_{3/2}$ fine structure interval in hydrogen has been measured to 1 part in 10^6. The experimental signal-to-noise ratio was high and the results were very reproducible. Subtracting this result from the theoretically well known $2P_{1/2}$-$2P_{3/2}$ field structure interval [1] calculated using [2] $\alpha^{-1}=137.0359895(61)$ yields an inferred measurement of the $n=2$ Lamb shift in hydrogen of 1057.839(12) MHz. This precision rivals that of previous direct measurements of the hydrogen $n=2$ Lamb shift [3–7]. Our result agrees best with the theoretical value of 1057.866(5) MHz [1,8] for which the proton radius was taken to be 0.805(11) fm [9–12]. The more recent value of the proton radius of 0.862(12) fm [13] results in a theoretical prediction of 1057.884(5) MHz [1,8] for the Lamb shift interval which does not agree as well with our result.

Figure 1 is a schematic drawing of the apparatus. Protons were created inside the accelerator by ionizing hydrogen in an RF discharge which was fed with 99.9995% pure H_2 gas. A magnet after the accelerator deflected the proton beam 30° and prevented ionized background gas in the source region from contaminating the beam. After exiting the accelerator region, fast hydrogen atoms were formed through charge exchange collisions of the proton beam with nitrogen gas. The atoms then passed through a state selection cavity, Doppler tuned onto resonance for the $2S_{1/2}(F=1)$-$2P_{3/2}(F=2)$ transition to preferentially quench the unwanted $2S_{1/2}(F=1)$ states. The cavity was 14.45 cm long in order to reduce transit time broadening of the RF which would have resulted in a substantial loss of population in the $2S_{1/2}(F=0)$ state. After exiting this cavity, the atoms passed through a second cavity which was used in conjunction with a background subtraction technique. Data were first taken with this prequench cavity off, then with it on. If this cavity only modulated the population in the $2S_{1/2}(F=0)$ state, the quantum mechanical signal of interest could have been isolated regardless of the population in the $2S_{1/2}(F=1)$ states. Using the state selection and prequench cavity it was possible to reduce the effective population in the $2S_{1/2}(F=1)$ states to less than 0.05% of the population in the $2S_{1/2}(F=0)$ state. The symmetry and center of the quench signal were extremely sensitive to population in the $2S_{1/2}(F=1)$ states, and fits of the quench signal over the wide 9.4–10.6 GHz range were used as a monitor of these state populations. Next the atoms entered the spectroscopy region where the actual SOF experiment was performed. The number of atoms in the $2S_{1/2}(F=0)$ and $2S_{1/2}(F=1)$ states after the spectroscopy region was detected by quenching these states with a dc field and monitoring the number of Lyman-α photons. All signals were normalized to the beam current which was monitored using a Faraday cup at the end of the beam line.

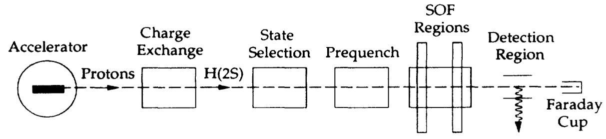

FIG. 1. Schematic drawing of the experimental apparatus.

The heart of the experiment was a magic tee optimized over the narrow frequency band of 9.85–10.15 GHz. Over this narrow band, it was possible to optimize the power division ratio and the phase relation between the microwaves exiting the output ports of the tee for both input ports. Using this tee the relative phase of the microwaves in the interaction regions was switched from 0 to π rad so that the quantum mechanical interference term could be isolated.

The signal source was phase locked using a locking counter and amplified using a traveling wave tube amplifier which generated the 37.6 V/cm (1.65 W at 10.03 GHz) needed in each interaction region. The output power of this amplifier was leveled to better than 1 part in 10^4 and was switched between the 0, off, and π configurations with a dwell time of 128 ms in each state using a SP3T coax switch and driver.

The separated oscillatory field technique used in this experiment has been described in detail elsewhere [7,14–17]. Using this technique, the linewidth of the transition can be significantly narrowed below the 100 MHz natural width imposed by the 1.6 ns lifetime of the P state. The SOF technique generates two relevant signals: the quench and interference signal. The quench signal is defined as the average percent depletion of the sur-

0031-9007/94/72(8)/1172(4)$06.00

viving $2S_{1/2}$ state populations when the microwave field is turned on with a relative phase of either 0 or π rad. The interference signal I is the difference in the depletion of the $2S_{1/2}$ state populations for relative microwave phases of 0 and π rad. The SOF interference signal is much less sensitive to ac Stark and Bloch-Siegert shifts than is the average quench signal, which roughly corresponds to a single field region experiment. Figures 2 and 3 show a typical data set for a 96.5 keV hydrogen beam. The average quench signal was sensitive to beam instabilities which caused the large error bars in one point in Fig. 2. Because the interference signal was the difference between the phase sensitive quench signals, it was not nearly as sensitive to these instabilities. Only the interference signals were used in the line center determination.

Data were taken in four configurations, two to eliminate any residual first order Doppler shift and two to eliminate any relative microwave phase error in the interaction regions. The Doppler shift was canceled by averaging measurements with the microwaves propagating in first one, then the other direction through the SOF regions. Residual phase errors were canceled by mechanically interchanging the interaction regions and the respective microwave components so that the time order of the beam through the interaction regions was reversed. The gross phase error due to path length differences from each output port of the magic tee to the center of the corresponding interaction region was reduced by using precision spacers. There was a spacer on each output arm of the magic tee, and each was machined to make the RF path lengths equal. Initially the spacers were machined so that the measured path lengths were equal, however, due to waveguide bends, it was not possible to do this accurately enough. The lengths were subsequently remachined according to experimental results which allowed proper determination of the RF path lengths. Using these spacers it was possible to reduce the shift in the interference center for phase inversion runs to the 100 kHz level. Doppler inversion interference center shifts were typically only 10 kHz due to the very stringent focus conditions on the atomic beam. A separate time of flight experiment was performed to measure the beam energy to 0.1% in order to determine the second order Doppler shift correction to a precision of 1 kHz.

Another source of phase error was reflection of the RF power incident on the directional couplers and imperfectly matched loads used to monitor the power leaving the interaction regions. Hewlett-Packard (HP) power meters were used to monitor directly the powers exiting the attenuated arms of each directional coupler assembly. The powers were set before data were acquired using a computer which cycled the RF switch with the same duty cycle used in the experiment in order to eliminate switch heating effects. The power meters were calibrated in this pulsed mode. The powers were also monitored during data acquisition and used to correct the raw signals. Specially designed X-band ceramic matched loads capable of withstanding over 10 W continuously in a vacuum were used as termination loads for the microwave powers. These matched loads had a typical voltage-standing-wave ratio (VSWR) of 1.02. The VSWR of the 30 dB directional coupler, matched load assemblies was typically 1.03. E-field reflections due to the VSWR's of these setups caused variations in the power and relative microwave phase in the interaction regions. The complex VSWR of each setup was measured as a function of frequency and these data were used to correct the input power to the interaction regions. The calibration of all microwave components is traceable to a single HP model 432A power meter and a single HP model X486A thermistor mount. These power measurement components were first calibrated by Hewlett-Packard using instrumentation that could be traced to a NIST standard. Phase errors resulting from load reflections would slightly distort the interference signal, resulting in an increased fit standard deviation. Such a distortion would invert sign for phase inversion pairs and, to first order, its effect on the line center would average out.

In previous SOF experiments using waveguides, a major error was due to the physical making and breaking of microwave joints between data runs. It was necessary to disassemble the microwave flanges before and after the interaction regions between each run. The microwave propagation direction had to be reversed in Doppler inversion runs and the microwave components also had to be disassembled in order to invert the interaction regions for the phase inversion runs. This random phase error

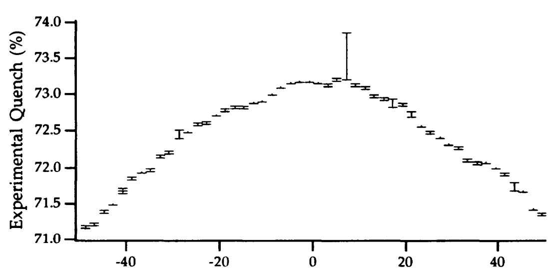

FIG. 2. Typical quench signal for a 96.5 keV beam with a field strength of 37.6 V/cm in each interaction region. The quench signal was only used to monitor the population in the $2S_{1/2}(F=1)$ states. No corrections were applied to these data.

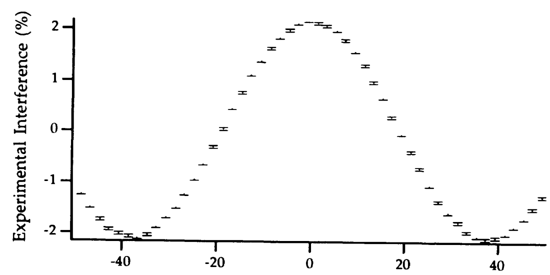

FIG. 3. Typical interference signal after corrections have been applied. Corrections were typically less than one-quarter the size of the error bars shown.

was eliminated by using alignment flanges that were accurately pinned together by two stainless steel pins. These special flanges improved the flange alignment precision by more than a factor of 20 over standard X-band flanges, thereby greatly reducing the random systematic errors that plagued previous experimenters. Every critical joint after the magic tee that had to be disturbed used these specially designed alignment flanges. Disassembling and reassembling all such joints typically resulted in less than a 3 kHz shift of the interference signal center which is consistent with the statistical standard deviation of several line-center fits in a given experimental configuration. Data taken as much as a week later in the same configuration also exhibited such reproducibility.

Cutoff tubes, made of oxygen-free high conductivity copper, allowed the atoms to enter while preventing microwave leakage from the interaction regions. The cutoff tubes between the interaction regions were 2.286 cm long and had an inside diameter of 0.476 cm for 1.397 cm, at which point they necked down to 0.318 cm for 0.889 cm (including the waveguide wall thickness of 0.127 cm). The cutoff tubes on the outer side of each interaction region were 2.667 cm long and had an additional 0.218 cm collimating aperture 0.127 cm thick before necking down to 0.318 cm. These apertures prevented atoms from interacting with the higher fields near the cutoff tube wall. Data were obtained as a function of cutoff tube length, revealing that the interference signal was extremely sensitive to any Doppler-shifted leakage field from these tubes.

Safinya *et al.* also measured the $2S_{1/2}$-$2P_{3/2}$ interval in hydrogen using an SOF technique, obtaining 9911.117(41) MHz [18]. The leakage fields escaping their interaction regions were measured before cutoff tubes were added [19]. Based on their measurements of the escaping field strength and the geometry of their cutoff tubes, the results of this experiment indicate that the cutoff tubes used in the experiment by Safinya *et al.* [18] were not adequate. We estimate that an additional correction of +0.102(30) MHz is appropriate which would shift their interval to 9911.219(51) MHz.

Simulations, which included all sixteen states in the $n=2$ manifold of hydrogen, were used to model the system and predict power shifts to the line center. The simulations directly integrated the Schrödinger equation for all electric field polarizations found in the waveguide and in the cutoff tubes. The cutoff tubes modified the boundary conditions of the waveguide and perturbed the dominant TE_{10} mode in the X-band interaction region. The actual field geometry was calculated on a finite grid subject to the boundary conditions of the experiment using the MAFIA supercomputer program at Brookhaven National Laboratory [20]. The simulations used these field strengths and polarizations to integrate the Schrödinger equation. Magnetic fields in the waveguide were included in the simulations through the motional $\mathbf{v}\times\mathbf{B}$ electric field they produced.

The simulations were used to model line-center shifts and optimize the experimental operating parameters. An optimal beam energy of 96.5 keV, for an interaction region separation of 4.610 cm, was selected to minimize the effects of population in the $2S_{1/2}(F=1)$ states upon the interference signal. At this energy the simulations predicted the interference signal would attain its maximum value at a field strength of 37.6 V/cm which corresponds to 1.65 W at 10.03 GHz. At this field strength the condition $\partial I/\partial P=0$ was satisfied, rendering the interference signal insensitive to power variations in the interaction regions. The measured interference signal was maximum at a field strength corresponding to 1.648(2) W at 10.03 GHz. For this reason all data were obtained at a field strength of 37.6 V/cm. Nonidealities such as population imbalances in the $2S_{1/2}(F=1)$ states, power imbalances in the interaction regions and errors in the state energies input to the simulations were systematically explored. Shifts in the interference and quench signals due to population in the $2S_{1/2}(F=1)$ states and the maximizing behavior of both signals as predicted by the simulations were verified experimentally, and in all cases agreement between simulations and experimental results was excellent.

Table I is a summary of corrections applied to the experimentally determined line center. A small correction due to incomplete quench subtraction was found by examining the average fit error after the residual phase errors were canceled. The total correction of −117.426(5) MHz was applied to the raw experimental interference line center of 10028.626(11) MHz, yielding an experimental value for the $2S_{1/2}$-$2P_{3/2}$ transition of 9911.200(12) MHz. The statistics were excellent as was the reproducibility of the experimental results. It would be possible to reduce the error bar in this experiment below the 10 kHz level by an improvement in the voltage standing wave ratio of the X-band microwave components used. Subtracting this experimental result from the theoretically well-known $2P_{1/2}$-$2P_{3/2}$ fine structure interval of 10969.0394(2) MHz [1] yields an inferred $2S_{1/2}$-$2P_{1/2}$ Lamb shift value of 1057.839(12) MHz. The re-

TABLE I. Summary of the corrections applied to the raw experimental line center.

Summary of corrections	
Source of correction	Value (MHz)
$F=1$ overlap	0.000(5)
Bloch-Siegert & ac Stark shifts	−0.069(1)
RF field slope	0.000(0)
Incomplete quench subtraction	−0.002(1)
Simulation input energy error	0.000(1)
Traveling waves in cutoff tubes	0.000(0)
Zeeman shifts	0.000(0)
Stark shifts	0.000(1)
Timebase error	0.000(0)
Time dilation	+1.031(1)
Hyperfine structure	−118.386(0)
Total corrections	−117.426(5)

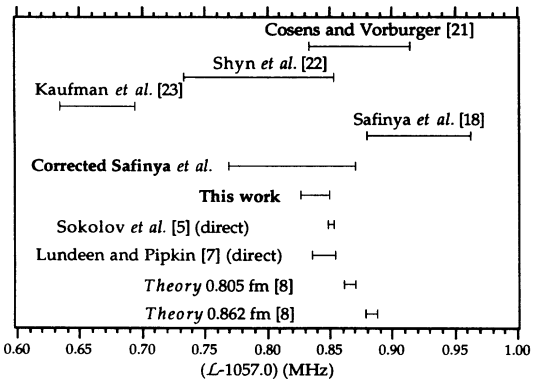

FIG. 4. A comparison between previous inferred Lamb shift measurements, the corrected result of Safinya *et al.* [18], this experimental result, the two most precise direct Lamb shift measurements, and theory. The lamb shift is denoted by $\mathcal{L}$.

ciprocal value of the fine structure constant used in the calculation of the $2P_{1/2}$-$2P_{3/2}$ interval was [2] $\alpha^{-1} = 137.0359895(61)$. Figure 4 compares this experimental result with the other indirect measurements of the Lamb shift [21–23] and with theory [1] for both values of the proton radius. The corrected result of Safinya *et al.* [18] and the two most precise direct measurements of the Lamb shift [5,7] are also included.

The two most precise direct measurements of the Lamb shift (see Fig. 4) are those of Palchikov, Sokolov, and Yakovlev [5], 1057.8514(19) MHz, and Lundeen and Pipkin [7], 1057.845(9) MHz. Our experimental result of 1057.839(12) MHz is in excellent agreement with these measurements and in fair agreement with the theoretical prediction of 1057.866(5) MHz [1,8], which was calculated assuming a proton radius of 0.805(11) fm [9–12]. The proton radius of 0.862(12) fm [13] results in a theoretical prediction of 1057.884(5) MHz [1,8] which is 3.5 combined standard deviations from this experimental result. This experimental result agrees best with the theoretical prediction based on the smaller proton radius, however, because of the discrepant values for the proton radius, one cannot make a definitive comparison between theory and experiment. Before an accurate comparison between theory and experiment can be made, the proton radius discrepancy must be resolved and higher order corrections to the Lamb shift must be calculated. Corrections of order $\alpha(Z\alpha)^6$ [24], $\alpha(Z\alpha)^5 m/M$ [25], and $(Z\alpha)^6 m^2/M$ [26] have already been calculated. Two loop binding corrections of order $\alpha^2(Z\alpha)^4$ and $\alpha^2(Z\alpha)^5$ have been calculated [27–29], but these results are not yet complete.

We would like to thank Dr. Martin Poitzsch for his help and many fruitful discussions during the course of this experiment. We would also like to acknowledge the support of the National Science Foundation through Grant No. PHY-9016886.

*Present address: Laboratoire de Spectroscopie Hertzienne de l'Ecole Normale Supérieure, 24 Rue Lhomond, 75231 Paris Cedex 05, France.
†Deceased.

[1] G. W. F. Drake, Phys. Rev. A (to be published).
[2] E. R. Cohen and B. N. Taylor, Rev. Mod. Phys. **59**, 1121 (1987).
[3] E. S. Dayhoff, S. Triebwasser, and W. E. Lamb, Jr., Phys. Rev. **89**, 106 (1953).
[4] R. T. Robiscoe and T. W. Shyn, Phys. Rev. Lett. **24**, 559 (1970).
[5] V. G. Palchikov, L. Sokolov, and V. P. Yakovlev, Lett. J. Tech. Phys. **38**, 347 (1983).
[6] G. Newton, D. A. Andrews, and P. J. Unsworth, Philos. Trans. R. Soc. London **290**, 373 (1979).
[7] S. R. Lundeen and F. M. Pipkin, Metrologia **22**, 9 (1986).
[8] A. Van Wijngaarden, J. Kwela, and G. W. F. Drake, Phys. Rev. A **43**, 3325 (1991).
[9] D. J. Drickey and L. N. Hand, Phys. Rev. Lett. **9**, 521 (1962).
[10] L. N. Hand, D. G. Miller, and R. Wilson, Rev. Mod. Phys. **35**, 335 (1963).
[11] B. Dudelzak, G. Sauvage, and P. Lehmann, Nuovo Cimento **28**, 18 (1963).
[12] D. Frerejacque, D. Benaksas, and D. Drickey, Phys. Rev. **141**, 1308 (1966).
[13] G. G. Simon, C. Schmitt, F. Borkowski, and V. H. Walther, Nucl. Phys. A **333**, 381 (1980).
[14] C. W. Fabjan and F. M. Pipkin, in *Proceedings of International Conference for Precision Measurement and Fundamental Constants, Gaithersburg, August 1970*, National Bureau of Standards Special Publication No. 343, edited by D. N. Langenberger and B. N. Taylor (U.S. GPO, Washington, D.C., 1971), p. 377.
[15] C. W. Fabjan and F. M. Pipkin, Phys. Lett. **36A**, 69 (1971).
[16] C. W. Fabjan and F. M. Pipkin, Phys. Rev. A **6**, 556 (1972).
[17] F. M. Pipkin, in *Quantum Electrodynamics*, edited by T. Kinoshita (World Scientific, Singapore, 1990), pp. 696–773.
[18] K. A. Safinya, K. K. Chan, S. R. Lunden, and F. M. Pipkin, Phys. Rev. Lett. **45**, 1934 (1980).
[19] K. A. Safinya, Ph.D. thesis, Harvard University, 1979 (unpublished).
[20] L. Moorman, SUNY Stony Brook, private communication with Protik Majumder.
[21] B. L. Cosens and T. V. Vorburger, Phys. Rev. A **22**, 591 (1980).
[22] T. W. Shyn, W. L. Williams, R. T. Robiscoe, and T. Rebane, Phys. Rev. Lett. **22**, 1273 (1969).
[23] S. L. Kaufman, W. E. Lamb, Jr., K. R. Lea, and M. Leventhal, Phys. Rev. A **4**, 2128 (1971).
[24] K. Pachucki, Ann. Phys. **226**, 1 (1993).
[25] G. Bhatt and H. Grotch, Ann. Phys. (N.Y.) **173**, 1 (1987).
[26] M. Doncheski, H. Grotch, and G. W. Erickson, Phys. Rev. A **43**, 2152 (1991).
[27] M. I. Eides, H. Grotch, and D. A. Owen, Phys. Lett. B **294**, 115 (1992).
[28] M. I. Eides and H. Grotch, Phys. Lett. B **301**, 127 (1992).
[29] K. Pachucki, Phys. Rev. A **48**, 2609 (1993).